International Journal of Biological Macromolecules 243 (2023) 125249

Contents lists available at ScienceDirect

International Journal of Biological Macromolecules

journal homepage: www.elsevier.com/locate/ijbiomac

A lubricant and adhesive hydrogel cross-linked from hyaluronic acid and chitosan for articular cartilage regeneration

Haofeng Qiu [a,b], Junjie Deng [b,c], Rufang Wei [b,c], Xiang Wu [b,d], Shengjia Chen [b,d], Yanyu Yang [b,c], Chenyang Gong [a], Lingling Cui [a], Zhangyong Si [e], Yabin Zhu [d], Rong Wang [b,*], Dangsheng Xiong [a,*]

[a] School of Materials Science and Engineering, Nanjing University of Science & Technology, Nanjing 210094, PR China
[b] Cixi Institute of Biomedical Engineering, Ningbo Institute of Materials Technology and Engineering, Chinese Academy of Sciences, Ningbo 315300, PR China
[c] Cixi Biomedical Research Institute, Wenzhou Medical University, Zhejiang 325035, PR China
[d] School of Medicine, Ningbo University, Ningbo 315211, PR China
[e] School of Chemical and Biomedical Engineering, Nanyang Technological University, Singapore 637459, Singapore

ARTICLE INFO

Keywords:
Polysaccharide hydrogel
Lubrication
Cartilage regeneration

ABSTRACT

Trauma-induced articular cartilage damages are common in clinical practice. Hydrogels have been used to fill the cartilage defects and act as extracellular matrices for cell migration and tissue regeneration. Lubrication and stability of the filler materials are essential to achieve a satisfying healing effect in cartilage regeneration. However, conventional hydrogels failed to provide a lubricous effect, or could not anchor to the wound to maintain a stable curing effect. Herein, we fabricated dually cross-linked hydrogels using oxidized hyaluronic acid (OHA) and *N*-(2-hydroxypropyl)-3-trimethylammonium chitosan chloride (HTCC) methacrylate (HTCCMA). The OHA/HTCCMA hydrogels, which were dynamically cross-linked and then covalently cross-linked by photo-irradiation, showed appropriate rheological properties and self-healing capability. The hydrogels exhibited moderate and stable tissue adhesion property due to formation of dynamic covalent bonds with the cartilage surface. The coefficient of friction values were 0.065 and 0.078 for the dynamically cross-linked and double-cross-linked hydrogels, respectively, demonstrating superior lubrication. *In vitro* studies showed that the hydrogels had good antibacterial ability and promoted cell proliferation. *In vivo* studies confirmed that the hydrogels were biocompatible and biodegradable, and exhibited a robust regenerating ability for articular cartilage. This lubricant-adhesive hydrogel is expected to be promising for the treatment of joint injuries as well as regeneration.

1. Introduction

Articular cartilage degeneration due to aging, trauma, or inflammation is prevalent in clinical practice nowadays [1]. Excessive exercise can also destroy articular cartilage and cause traumatic arthritis, which can seriously impair the ability to walk [2]. Due to the lack of lymphatic, nerve, or blood supply to the articular cartilage, the chondrocytes obtain nutrients through intra-stromal diffusion from the subchondral blood vessels and surrounding tissue fluid [3–5]. The extracellular matrix of the chondrocytes restricts the ability of those undifferentiated cells that can repair articular cartilage damage to migrating to the defective area, resulting in poor self-healing, and these defects or injuries persist for years before eventually leading to arthritis [6].

Restoration of the lubrication function and repair of the damaged cartilage are important for the treatment of traumatic arthritis [7,8]. Typically, patients with osteoarthritis receive their initial hyaluronic acid supplementation therapy through injections of a single hyaluronic acid matrix in the joint cavity [9], which only offers a limited degree of lubrication aid. Simple hyaluronic acid would be completely degraded and absorbed by the body in about a week because it cannot endure the harsh conditions of high frequency and high load on the joint [10].

To address this problem, scientists envisioned filling cartilage defects with a construct such as a hydrogel, which functions similarly to an extracellular matrix to hold cells in place and retain the space for tissue growth, thereby allowing the defective cartilage to regenerate [11–13]. Hydrogels have been proven promising because they closely resemble

* Corresponding authors.
E-mail addresses: rong.wang@nimte.ac.cn (R. Wang), xiongds@njust.edu.cn (D. Xiong).

https://doi.org/10.1016/j.ijbiomac.2023.125249
Received 15 February 2023; Received in revised form 16 May 2023; Accepted 6 June 2023
Available online 7 June 2023

the natural extracellular matrix, thus providing a three dimensional culture microenvironment that is conducive to encapsulating cells to maintain a rounded morphology and cartilage-forming phenotype [6,14,15]. In addition, hydrogels enable high cell inoculation density and uniform cell distribution across the scaffold. They also provide external stimuli to the embedded cells to guide regenerative cartilage growth and formation [16]. However, conventional hydrogels are difficult to handle and fabricate into cartilage regeneration structures with the desired internal structure and exterior shape due to their poor mechanical strength [17]. Moreover, most of hydrogels lack lubrication properties, and the frictional shear forces within the joint during the repair process can easily lead to breakage of the cartilage friction interface. In addition, they also have a tendency to detach from tissue defects due to the lack of appropriate adhesiveness [18]. Lastly, conventional hydrogel lacks antimicrobial activity to reduce the risk of bacterial infection during joint therapy. To overcome these problems, further research on injectable hydrogels with lubrication properties, appropriate mechanical properties, adhesive capability and antimicrobial properties is needed.

Compared to synthetic polymers, natural polymers like hyaluronic acid (HA) and chitosan have good biocompatibility and biodegradability [19,20]. Introduction of natural polymers into the hydrogel helps to improve their bioactivity. HA is one of the main components of synovial fluid, produced by articular chondrocytes and synovial cells, and released into the joint cavity where it accumulates on the surface of cartilage and ligaments, playing a major role in joint lubrication and maintaining intra-articular homeostasis [21,22]. In addition, HA can contribute to fibroblast proliferation and collagen synthesis, as well as to the synthesis of proteoglycans in degenerating chondrocytes. *In vivo* study indicates that HA is involved in regulating cell motility and promoting cell migration, and it also interacts with the cell surface receptor CD44 to regulate the accumulation and formation of extracellular matrix [23,24]. On the other hand, chitosan, as a cationic polymer containing a large number of amino groups, is widely used in wound healing applications, and quaternized chitosan has good antimicrobial properties to inhibit wound infections caused by trauma [25,26].

This study aimed to prepare lubricating hydrogels with specific tissue adhesiveness and antibacterial properties for the regeneration of articular cartilage and the prevention of joint lesions. The hydrogels were composed of oxidized HA (OHA) and *N*-(2-hydroxypropyl)-3-trimethylammonium chitosan chloride (HTCC) methacrylate (HTCCMA), called OHA/HTCCMA hydrogels. The dynamic hydrogel was first fabricated by Schiff base reaction between the aldehyde group in OHA and the amino group in HTCCMA. The dual cross-linked hydrogel with high mechanical property was then obtained through covalently cross-linking of the dynamic OHA/HTCCMA hydrogel. In addition, there is a large amount of glycosaminoglycan in cartilage [27], which could react with the aldehyde group in the OHA of the hydrogel, together with the electrostatic interactions and hydrogen bonding between the interface, to anchor the hydrogel onto the cartilage. The formulation of the hydrogel was adjusted, and the rheology, degradation, lubrication, tissue adhesion, and antimicrobial properties of the hydrogels were characterized. In addition, the biocompatibility of OHA/HTCCMA hydrogels was systematically investigated by culturing with rabbit articular chondrocytes and mesenchymal stem cells as well as by subcutaneous implantation *in vivo*. Finally, the optimized OHA/HTCCMA hydrogel was used for treatment of total articular cartilage defects in a rabbit model. Wound morphology and histological changes were analyzed to assess the potential of the OHA/HTCMA hydrogel in cartilage regeneration.

2. Material and methods

2.1. Materials

Chitosan (high viscosity >400 mPa•s, deacetylation degree = 91.99 %), sodium periodate, methacrylic anhydride, and glycidyltrimethylammonium chloride were purchased from Aladdin Chemistry (Shanghai, China). Hyaluronic acid (molecular weight: 1,800,000 Da) was purchased from Bloomage Biotechnology (Jinan, China). *Staphylococcus aureus* (*S. aureus*) 5622 was a gift from the Affiliated Hospital of the School of Medicine of Ningbo University. *Escherichia coli* (*E. coli*) ATCC 25922 was obtained from American Type Culture Collection. Rabbit articular chondrocytes and rabbit bone marrow mesenchymal stem cells were purchased from Procell Life Science & Technology (Wuhan, China).

2.2. Polymer synthesis

Three grams of hyaluronic acid was dissolved in 300 mL of deionized water at room temperature, and 1.0 g of sodium periodate was added to the hyaluronic acid solution to initiate the reaction in dark. After 4 h, 0.5 mL of ethylene glycol was added to the solution to react with the excess sodium periodate. After 2 h, the solution was collected and subjected to dialysis using a cellulose membrane (molecular weight cut-off: 8000–14,000 Da) for 7 days, and freeze-dried to obtain OHA powder.

N-(2-hydroxypropyl)-3-trimethylammonium chitosan chloride (HTCC) was synthesized based on reported studies with slight modifications [28]. One gram of chitosan was dispersed in 36 mL of 0.5 % v/v aqueous acetic acid solution at room temperature. After the chitosan powder was fully dissolved, 1.425 g of glycidyltrimethylammonium chloride was added to the solution, and the reaction proceeded at 55 °C for 18 h. The reaction solution was centrifuged at 7000 r/min for 10 min, and the supernatant was removed. The resultant product was dialyzed in deionized water for 7 days using a cellulose membrane (molecular weight cut-off: 8000–14,000 Da), and freeze-dried to obtain HTCC powder.

HTCC methacrylate (HTCCMA) was prepared by adding 2 mL methacrylic anhydride into 300 mL of HTCC aqueous solution (containing 2 g of HTCC). The reaction proceeded at 60 °C for 3 h. Finally, the product was dialyzed using a cellulose membrane (molecular weight cut-off: 8000–14,000 Da), and freeze-dried to obtain HTCCMA powder.

The synthesized polymers were characterized using Fourier transform infrared (FTIR) spectroscopy (Nicolet-iS50 spectrometer, Thermo Scientific), and ^{1}H Nuclear magnetic resonance (^{1}H NMR, Bruker Ascend 400 MHz, with deuterated water and deuterated acetic acid as the solvents and internal standards).

2.3. Polymer characterization

The degree of oxidation of HA was determined by the reaction of the aldehyde group with hydroxylamine hydrochloride [29]. One hundred milligram of OHA powder was dissolved in 25 mL of hydroxylamine hydrochloride solution (0.25 mol/L, containing 0.0003 wt% methyl orange reagent) and stirred at 25 °C for 24 h. The hydrochloric acid released by the reaction was titrated with 0.1 mol/L sodium hydroxide solution until the red-to-yellow transition point was reached. The degree of oxidation of OHA was calculated according to the equation below:

$$\text{Oxidation degree}\% = 403c \times V \times 10^{-3}/2w$$

Where 403 is the molecular weight of saccharide repeating unit (g/mol); c is the concentration of sodium hydroxide solution (mol/L); V is the volume of sodium hydroxide solution consumed (mL); and w is the weight of OHA (g).

2.4. Hydrogel preparation

HTCCMA solution was prepared by dissolving 2 g HTCCMA powder in 100 mL of 1 wt% $CaCl_2$ solution to achieve a concentration of 2 %. OHA solution was prepared in serial concentrations of 4 %, 6 %, and 8 %. The two polymer solutions were mixed in equal volumes, to obtain

hydrogels of O_4H_2, O_6H_2, and O_8H_2, respectively, *via* the Schiff base reaction between the amino groups of HTCCMA and the aldehyde of OHA. In addition, 0.2 wt% lithium phenyl-2,4,6-trimethylbenzoylphosphinate (LAP) initiator was added to the polymer solutions before mixing, and the mixture was irradiated with 405 nm excitation light for 3 min to obtain dually cross-linked hydrogels of O_4H_2D, O_6H_2D, and O_8H_2D.

The obtained hydrogels were freeze-dried and fractured with liquid nitrogen, and the cross-sections of the hydrogels were observed with a scanning electron microscope (SEM, Regulus 8230, Hitachi, Japan).

2.5. Deswelling ratio, degradation rate and HA release

Hydrogel samples (15 mm × 15 mm × 5 mm) were incubated in 10 mL of phosphate buffered saline (PBS, 10 mM, pH 7.4) at room temperature for a determined period of time. Excess water was removed from the surface of the hydrogel with filter paper, and the remaining hydrogel was weighed and recorded. The deswelling ratio (DSR) of the hydrogel was calculated according to the following equation:

$$DSR = W_t/W_0 \times 100\%$$

where DSR is the deswelling ratio, W_0 and W_t are the weights of hydrogel before and after immersion.

To measure the degradation rate, hydrogel samples (15 mm × 15 mm × 5 mm) were immersed in 10 mL of PBS solution with or without 100 U/mL of hyaluronidase at room temperature. At pre-determined points of time, the hydrogel was collected, freeze-dried, and the remaining mass was weighed. The mass remaining ratio (MR) of the hydrogel in PBS or hyaluronidase solution was calculated according to the following equation:

$$MR = M_t/M_0 \times 100\%$$

Where MR is the mass remaining ratio after degradation, M_0 and M_t are the mass of hydrogel before and after degradation.

HA concentration was determined by the carbazole-sulfuric acid method. Briefly, hydrogel sample (15 mm × 15 mm × 5 mm) was placed in 15 mL of PBS, and 1 mL of the leachate was drawn into a glass test tube at pre-determined points of time, and placed in an ice-water bath. Five mL of sodium tetraborate sulfate solution (0.025 mol/L) was slowly added to the tube with an acid burette, mixed well and placed in a boiling water bath for 20 min. After cooling to room temperature, 0.2 mL of 0.1 % carbazole ethanol solution was added to the mixture, which was shaken well and allowed to stand at room temperature for 2 h. The absorbance of the solution at 550 nm was measured by UV spectrophotometer (Agilent, cary300) at room temperature, and the amount of HA released was calculated using the standard curve.

2.6. Rheology characterization, self-healing property, texture analysis and water contact angle

The rheological characterization of the hydrogel was tested using a rotational rheometer at 25 °C. The OHA and HTCCMA polymer solutions were mixed in equal volumes in a syringe, and the mixture was extruded as a continuous filament gel to the measuring plate. The storage modulus (G′) and loss modulus (G″) of the hydrogel were measured by strain amplitude experiment (γ = 0.1 % - 1,000.0 %) at a fixed angular frequency (10.0 rad/s). The viscosity of the hydrogel at different shear rates (0.1–30 1/s) was recorded. To investigate the self-healing property of the hydrogels, the G′ and G″ of hydrogel sample switching between a small strain (γ = 1.0 %) and a large strain (γ = 1,000.0 %) at a fixed angular frequency (10.0 rad/s) with the alternative step of strains every 60 s were recorded. Hydrogel sample (15 mm × 15 mm × 5 mm) was cut into two halves, and recombined together at room temperature.

Texture analysis (BosinTech, China) was performed using a hold test by injecting 2 mL of hydrogel into a 24-well plate and holding it steadily for 60 s after pressing down with the probe at a rate of 0.5 mm/s for 5 mm, and the final hold residual force of the hydrogel was used as the determination of the gel strength. The water contact angle (KRUSS, DSA25) was tested by first forming a thin layer of hydrogel on a glass slide by spin coating method. A droplet of water was dropped on the surface of the hydrogel and the contact angle of the droplet was tested after stabilization for 1 min.

2.7. Friction test

Freshly slaughtered porcine femur bones were purchased from a local market and washed with PBS to remove the synovial fluid on the cartilage surface to prevent interference with the experiment. A cylindrical bone containing the cartilage layer with a diameter of 4 mm and a height of 1 cm (cartilage thickness of ~1.5 mm) was drilled out from the femoral head location using a bone opener. A custom-made fixture was used to fix the cylindrical bone with the cartilage part exposed as the friction head, and a polished titanium plate was selected as the base plate. The raw material of titanium sheet was wire cut and polished with 240, 320, 400, 600, 800, 1,000, 1,200 and 1,500 mesh in sequence, and finally polished with 15,000 abrasive paste to obtain the titanium sheet base plate for the test.

The coefficient of friction (COF) of the cartilage on titanium plate in the absence or presence of the hydrogel sample was measured using a UTM Bruker TriboLab pin-on-plate tribometer (Bruker, Germany). The loading force of the cartilage onto the titanium plate was set to 10 N. The setup was stabilized for 30 s, and the test started with a reciprocal sliding speed was 10 mm/s at a stroke of 10 mm for 450 cycles.

2.8. Adhesion test

A hole of 5 mm in diameter and 1 mm in depth was drilled at the surface of the porcine femoral head. The hydrogel was squeezed into the defect using a syringe. The femur was immersed in PBS (10 mM, pH 7.4 or 6.4) at room temperature to investigate the stability of hydrogel adhesion on cartilage in an aqueous environment. The adhesion strength of hydrogel to cartilage was quantified using the lap shear method. Briefly, a 10 mm × 10 mm × 1.5 mm cartilage tissue was cut from the flat part of the medial and lateral femoral condyles of the femur (without or with rub by sandpaper to mimic an arthritic surface), and glued to a titanium sheet so that its two pieces of cartilage tissue were parallel to each other. Two pieces of the cartilage were fixed face to face using a piece of hydrogel (10 mm × 10 mm × 1.5 mm). Tensile tests were performed using a Universal Testing Machine (CMT-1104, SUST, China) to measure the adhesion strength of the hydrogel to cartilage at a crosshead speed of 20 mm/min.

2.9. Antibacterial assay

Overnight bacterial cultures were collected by centrifugation and diluted with sterilized PBS (10 mM, pH 7.4) to a bacterial suspension concentration of 4×10^5 CFU/mL. Hydrogel sample (15 mm × 15 mm × 5 mm) was placed in 10 mL of the bacterial suspension and incubated with shaking at 37 °C. At time points of 6, 12 and 24 h, 100 μL of the suspension was aspirated. Viable bacterial cells in the suspension were counted by the spreading plate method, as described in the previous study [30].

2.10. Cytotoxicity and hemolysis assays

Rabbit articular chondrocytes (CP002) and primary bone mesenchymal stem cells (BMSC) were selected in this study, and DME/F12 medium (supplemented with 10 % bovine serum) and RPMI medium (supplemented with 10 % bovine serum) were used for the culture of CP002 and BMSC, respectively. Hydrogel extracts were obtained by incubating 2 g of hydrogel in a 15 mL centrifuge tube containing 10 mL

of medium (ratio of hydrogel weight to medium volume: 200 μg/mL) for 24 h in a 4 °C refrigerator. In each well of the 96-well plate, 10 μL of cell suspension at a concentration of 7×10^5 cells/mL was added, and a certain amount (10, 20, 30, 40, and 50 μL) of the hydrogel extract was added to each well, respectively. The final volume of medium in each well was supplemented to 100 μL with culture medium. Therefore, the ratios of hydrogel weight to medium volume of the extract medium in each group were 20, 40, 60, 80, and 100 μg/mL, respectively. The cells were incubated at 37 °C with 5 % CO_2 for 72 h. The original medium was discarded, and 100 μL of fresh medium and 10 μL of CCK8 solution was added to each well. The cell viability of each group was measured and calculated following the instruction of the CCK8 assay.

For the cell proliferation assay, 10 μL of cell suspension at a concentration of 3×10^5 cells/mL was added to each well of a 96-well plate, followed by addition of 20 μL of the hydrogel extract medium, and the final volume was supplemented with culture medium to 100 μL in each well. The cells were incubated at 37 °C and 5 % CO_2 for 7 days (culture medium was replaced with medium containing the same ratio of hydrogel extract every two days). The cell viability of each group was measured using the CCK-8 assay as described above. The live/dead test using the Calcein/P Cell Viability and Cytotoxicity Assay Kit (Beyotime, China) was conducted to observe the survival status of cells visually using a fluorescence microscope (Nikon, TS2R-FL).

Ten mL of physiological saline (0.9 % NaCl) was added to 8 mL of fresh anticoagulated rabbit blood to obtain diluted anticoagulated free blood following the standard protocol [31]. A hydrogel sample weighed at 5 g was placed in a 15 mL centrifuge tube, and 10 mL of saline was added to fully cover the hydrogel. For the negative control group, only 10 mL of physiological saline was added, and for the positive control group, 10 mL of 1 % Triton X-100 was added. After incubating in a 37 °C water bath for 30 min, 0.2 mL of the diluted anticoagulated free blood was added, and it was incubated for another 60 min. The suspension was centrifuged and the absorbance of the supernatant at 545 nm was measured using a UV–Vis spectrometer (Agilent, Cary300).

2.11. In vivo hydrogel degradation and cartilage repair

New Zealand White rabbits (female, ~3 kg, 3–4 months) were used in this study. The animal experiments were performed in compliance with the principles of the National Research Council's Guide for the Care and Use of Laboratory Animals, and Laboratory animal - Guideline for ethical review of animal welfare (GB/T 35892-2018), and approved by the Institutional Animal Ethical Committee of Ningbo University.

After the animal was anaesthetized, 1 mL of the pre-gel mixture or the photo-cross-linked hydrogel was implanted subcutaneously in the rabbit's back. The rabbits were sacrificed on Days 1, 7, 14, 21, and 28. The buried location was exposed for photography after the full skin layer was removed. The skin tissue was embedded with paraffin, sectioned, and stained using hematoxylin and eosin (H&E) for observation.

For the cartilage repair experiment, after the animal was anaesthetized, the rabbit's knee joint was shaved and disinfected with an alcohol swab. The joint skin and the internal cruciate ligament were cut open, and a full-layer defect of 3 mm in diameter and 5 mm in depth was created in the rabbit's femoral trochlea using a bone opener. The defect was filled with hydrogel through syringe injection, and cross-linked by photo-irradiation at 405 nm for 2 min. The wound area was sutured, and the animal was fed following the protocol. In the control group, the defect in the animal femoral trochlea was left untreated. The rabbits were sacrificed on Days 1, 14, 28, 42, and 56, and the femur was collected and photographed for observation. The tissue was embedded by the paraffin, sectioned, and stained for observation.

2.12. Statistical analysis

Results were reported as the mean ± standard deviation of at least three samples per group. A *t*-test was used to determine the statistical significance between groups (accepted at $p < 0.05$).

3. Results and discussion

3.1. Polymer characterization

OHA was synthesized *via* oxidation of the vicinal hydroxyl groups on the HA unit ring by sodium periodate (Fig. 1A). A characteristic absorption peak at 1736 cm^{-1}, which can be attributed to the stretching vibration of the aldehyde carbonyl group of OHA, was observed in the FTIR spectrum (Fig. S1A). The resonance signals at 9.50 ppm and 4.88 ppm in the ^1H NMR spectrum correspond to the protons of the aldehyde group of OHA (Fig. S1B). The degree of oxidation of OHA was determined to be 26.20 % *via* the hydroxylamine hydrochloride titration assay.

HTCC was synthesized *via* a reaction of amino groups on the chitosan unit ring with glycidyltrimethylammonium chloride (Fig. 1B). In the FTIR spectrum of HTCC, the absorption peak at 1598 cm^{-1}, which was attributed to the secondary amine group on the chitosan backbone, decreased due to partial consumption of the anime groups in the HTCC synthesis (Fig. S1C). A new peak at 1478 cm^{-1} appeared due to the introduction of the quaternary ammonium group in the polymer. A strong stretching vibration at 1544 cm^{-1}, which was the characteristic peak of the carbon-carbon double bond, was observed in the spectrum of HTCCMA. The peak at 1478 cm^{-1} remained in the spectrum, indicating the successful introduction of both methacrylate group and quaternary ammonium group in the polymer. The signals at 3.14 ppm in the ^1H NMR spectrum can be attributed to protons of the quaternary ammonium group, and the signals between 5.55 ppm and 5.68 ppm can be attributed to the protons of the methacrylate group, respectively, also confirming the successful preparation of HTCCMA (Fig. S1D). From the ^1H NMR results, it can be calculated that the grafting efficiency of quaternary ammonium group was 9.46 %, and the degree of methacrylation was 7.49 % (Fig. S2). The details of the calculation are described in the Supporting Information.

3.2. Characterization of OHA/HTCCMA hydrogels

Considering the degree of functionalization of OHA and HTCCMA, and the steric hindrance effect of the two adjacent aldehyde groups in OHA molecule, the mass ratios of OHA to HTCCMA at 4:2, 6:2, and 8:2 were selected for the hydrogel preparation in the study. The two polymer solutions were mixed in equal volumes to form a dynamic hydrogel *via* the Schiff base reaction of amino groups in HTCCMA and aldehyde groups in OHA, and then the methacrylate groups in HTCCMA were cross-linked by photo-irradiation to obtain a dual-cross-linked hydrogel (Fig. 1C). From the SEM images, it was observed that the hydrogels before and after cross-linking by photo-irradiation showed porous internal structure with comparable pore size (Fig. 2A). The hydrogels after covalent cross-linking had thicker pore walls, compared to the one without photo-irradiation. This was probably due to the covalent cross-linking by methacrylate groups in HTCCMA, which resulted in high mechanical property and may be beneficial for cartilage regeneration applications.

The swelling/deswelling properties of hydrogels are important in the cartilage repair application, as excessive swelling effect of hydrogel may cause damage to the surrounding tissues by squeezing, and reduce the overall mechanical strength of the hydrogel. In contrast, deswelling may cause the hydrogel to detach from the tissue defect. The swelling/deswelling ratio of the hydrogels until the equilibrium state was investigated (Fig. 2B). It can be seen that all the OHA/HTCCMA hydrogels deswelled in PBS, and almost reached the equilibrium state after 360 min. The deswelling behavior of the OHA/HTCCMA hydrogels was gradually inhibited with the increase of OHA content in the hydrogel (the final deswelling ratio was 16.83 % of O_4H_2, 19.44 % of O_6H_2, and 25.68 % of O_8H_2). The dually cross-linked hydrogel deswelled at a lower

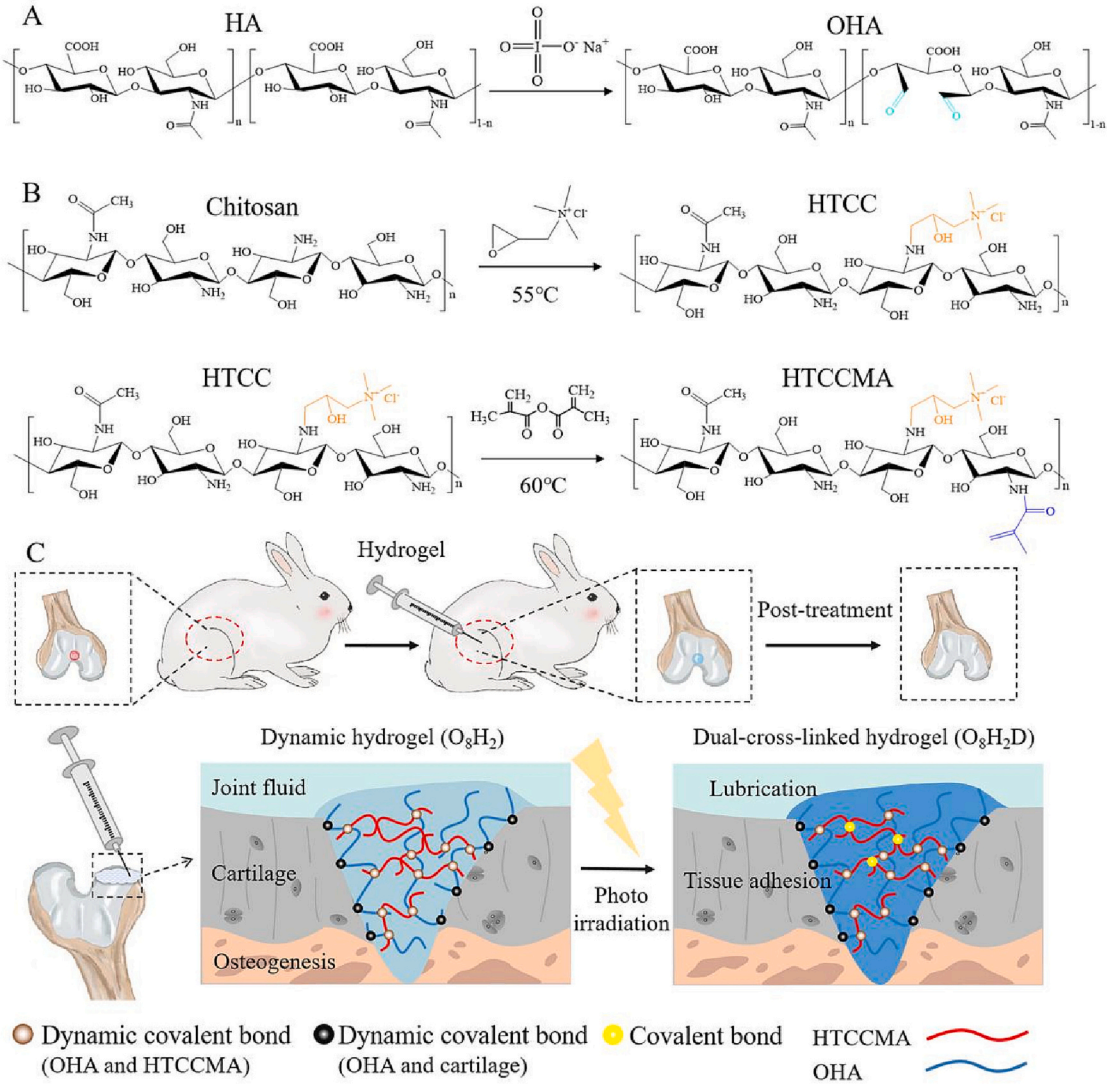

Fig. 1. Schematic diagram illustrating A) synthesis of OHA, B) HTCCMA, and C) preparation of dual-cross-linked OHA/HTCCMA hydrogel for articular cartilage reparation.

extent compared to the dynamic cross-linked counterpart, indicating that the hydrogels cross-linked by dually covalent bonds and dynamic bonds had stronger spatial networks and could inhibit the deswelling effect of hydrogels.

In addition, the degradation rate of hydrogels is also an important aspect of concern, as conventional hyaluronic acid injection often poses a great burden to patients in osteoarthritis treatment because of its rapid degradation rate. In this work, the degradation of hydrogels in the presence or absence of hyaluronidases over 28 days was investigated (Fig. 2C and D). In PBS buffer without hyaluronidase, the degradation loss of O_6H_2 was higher than those of O_8H_2 and O_4H_2. The degradation loss of the hydrogel was inhibited by photo-cross-linking, and the mass remaining after 28 days of degradation were 28.55 % for O_4H_2D, 25.30 % for O_6H_2D, and 26.14 % for O_8H_2D, respectively. With hyaluronidase in the buffer, the degradation rates of all the hydrogels increased, and the overall degradation loss was greater than that in the absence of the enzyme. The covalent cross-linking treatment also showed an inhibitory effect against the hyaluronidase degradation of the hydrogels. This indicates that the dual cross-linking system could resist the action of hyaluronidase, and can potentially prolong the *in vivo* efficacy of the hydrogels in osteoarthritis treatment. In addition, HA continuously released from the hydrogels over 21 days (Fig. 2E). The three formulations of hydrogels performed similarly in terms of deswelling ratio, degradation rate, pore size, and HA release profile. Considering that O_8H_2 and O_8H_2D hydrogels contain higher OHA contents, they may provide more reactive groups for the Schiff base reaction with glycosaminoglycans in the cartilage tissue for tissue adhesion, and more bioactivity for cartilage reparation. Therefore, O_8H_2 and O_8H_2D hydrogels were selected for the rest of the study.

3.3. Rheological properties self-healing behavior, texture analysis and water contact angle of hydrogels

The rheological properties of the hydrogels were examined using a rotational rheometer. A significant increase in storage modulus (G') was observed when the O_8H_2 hydrogel was cross-linked by photo-irradiation, indicating that the formation of covalent cross-linking significantly enhanced the mechanical property of the hydrogel (Fig. 3A). The storage modulus (G′) and loss modulus (G") of the O_8H_2 hydrogel at the strain amplitude range of 0.1 % to 1,000.0 % were scanned (Fig. 3B), and the results showed that the hydrogel was able to undergo the transition from gel to sol state at $\gamma = 623$ %. The viscosity of the O_8H_2 hydrogels decreased as the shear rate increased from 0.25 1/s to 30 1/s (Fig. 3C), reflecting a shear thinning nature of the hydrogel at high shear rates, which is beneficial to be used as an injectable hydrogel in the minimally invasive surgery for cartilage repair. The G′ and G" of

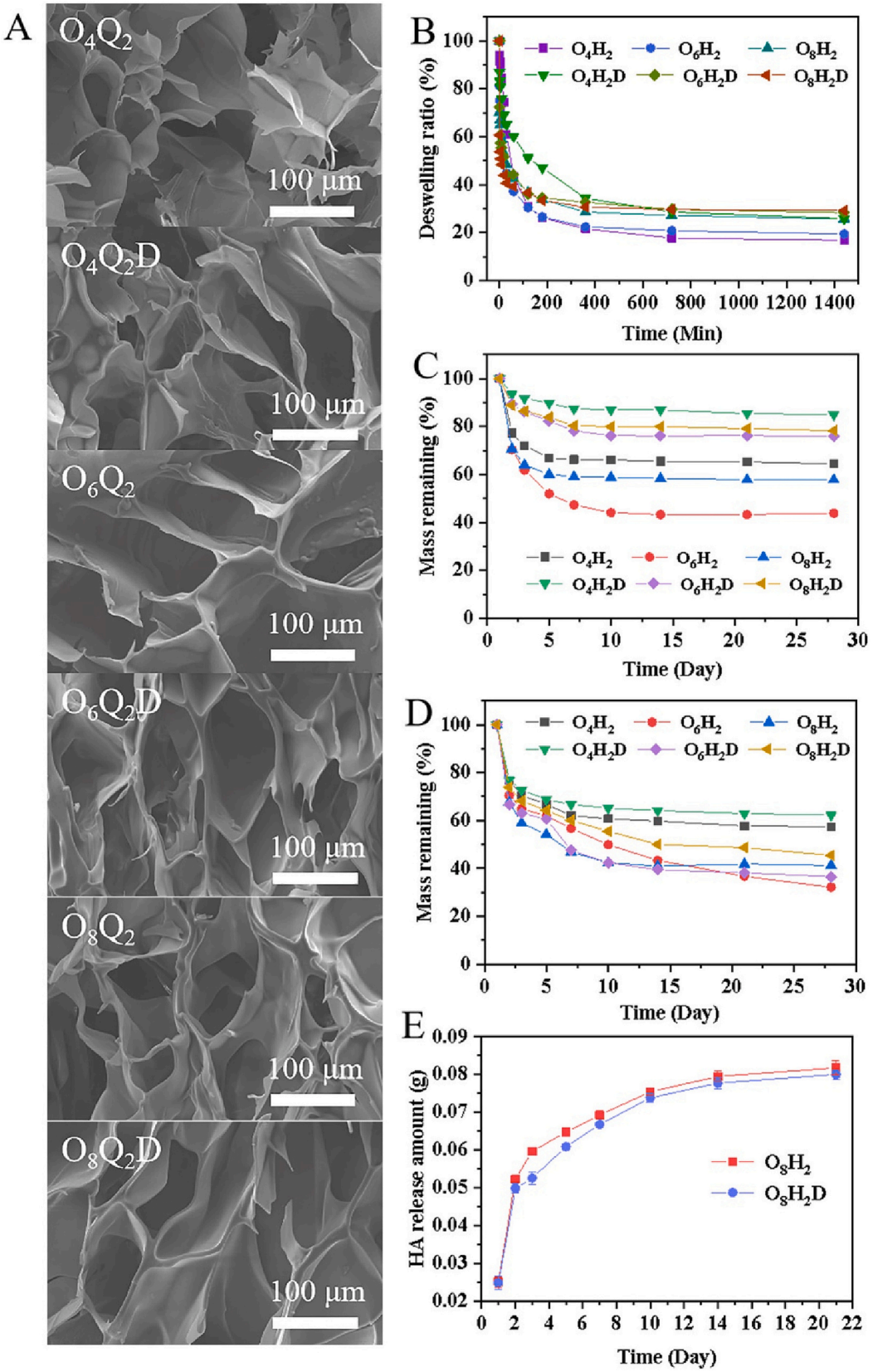

Fig. 2. Characterization of hydrogels. A) Cross-section of OHA/HTCCMA hydrogels. B) Deswelling ratio of OHA/HTCCMA hydrogels in PBS (n = 3). C) Mass remaining of OHA/HTCCMA hydrogels in PBS (n = 6). D) Mass remaining of OHA/HTCCMA hydrogels in PBS with 100 U/mL hyaluronidase (n = 3). E) Release of HA from hydrogel (15 mm × 15 mm × 5 mm) in 15 mL PBS over 21 days (n = 5).

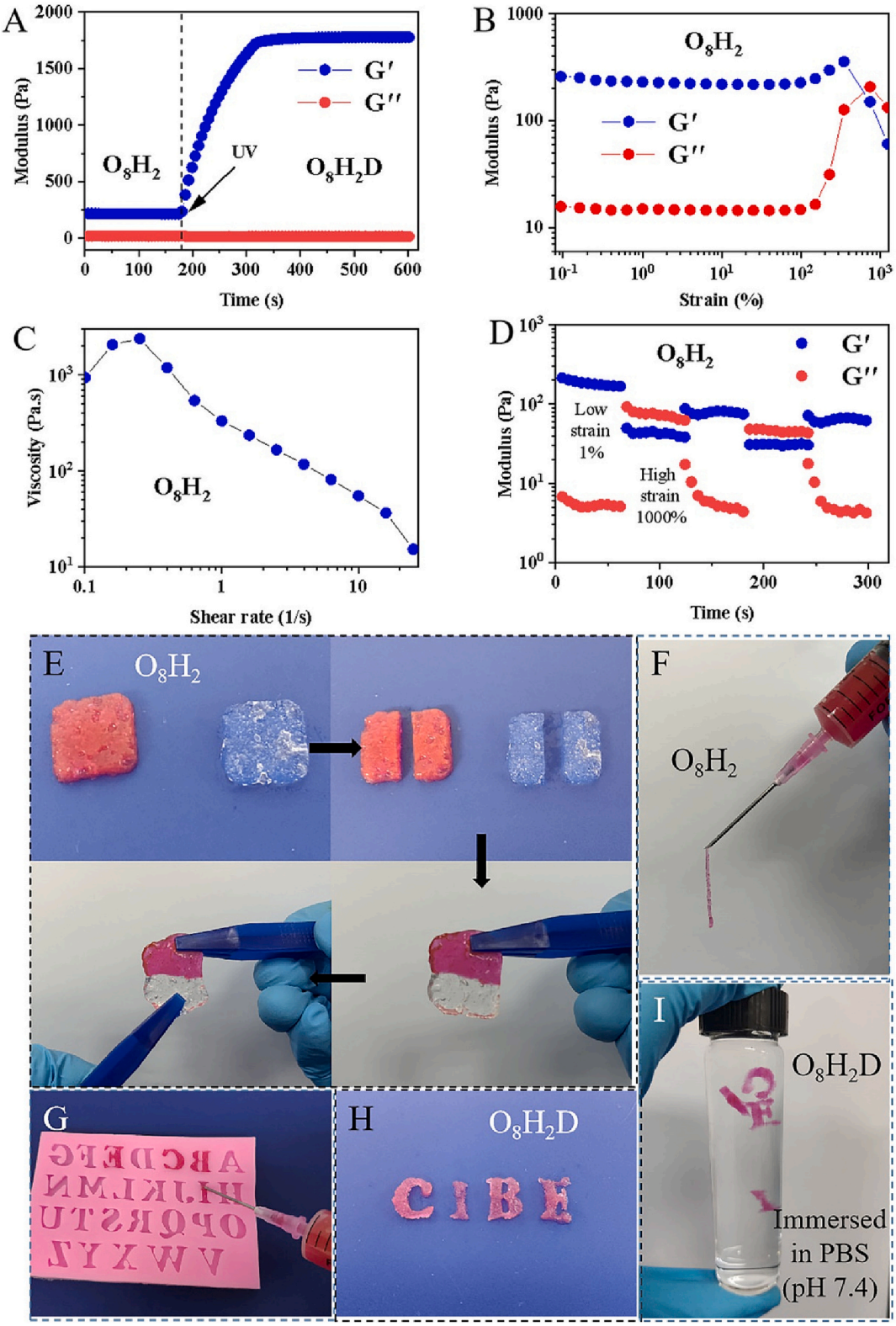

Fig. 3. Rheological properties of hydrogels and their macroscopic self-healing behavior and injectability. A) Time sweep of O_8H_2 hydrogel cross-linked by photo-irradiation to form O_8H_2D hydrogel. B) G′ and G″ of O_8H_2 hydrogel from strain amplitude sweep (γ = 0.1 %–1,000.0 %) at a fixed angular frequency (10.0 rad/s). C) Viscosity variation of O_8H_2 hydrogel at different shear rates (0.1–30 1/s). D) Alternating step strains when G′ and G″ of O_8H_2 hydrogel were switched from small strain (γ = 1.0 %) to large strain (γ = 1,000.0 %) at a fixed angular frequency (10.0 rad/s). E) O_8H_2 hydrogel was cut into two halves (one stained with red dye) and re-healed. F) O_8H_2 mixture was loaded into a syringe, and squeezed out as a continuous filamentous hydrogel; G-I) O_8H_2 hydrogels were squeezed into "C", "I", "B", "E" letters and cross-linked by photo-irradiation to form O_8H_2D hydrogels, and the O_8H_2D hydrogels remained stable in PBS (pH 7.4) over 60 days.

the O_8H_2 hydrogel at a small strain (γ = 1.0 %) and a large strain (γ = 1,000.0 %) at a fixed angular frequency (10.0 rad/s) showed that the hydrogel could completely interconvert between the sol state and the gel state even after the drastic strain (Fig. 3D), demonstrating its excellent self-healing performance, which is inseparable from the contribution of the dynamic cross-linking structure in the hydrogel. The self-healing behavior of the hydrogel was also visually observed by connecting two pieces of O_8H_2 hydrogel (one of which was stained with red dye), which were healed together within 1 min, and it was not easy to separate the hydrogels by pulling with tweezers (Fig. 3E). Thanks to the excellent shear-thinning and self-healing properties, the hydrogel can be easily injected from a surgical syringe (Fig. 3F), and form various shapes in a mold (Fig. 3G and H). The O_8H_2D hydrogel formed by photo-induced cross-linking showed excellent stability *in vitro*, and maintained its original shape after incubation in PBS for 60 days (Fig. 3I). The texture analysis showed that the retention residual force of the hydrogel increased from 7.80 gf for O_8H_2 to 26.43 gf for O_8H_2D after cross-linking (Fig. S3), indicating that the mechanical strength of the hydrogel after chemical cross-linking has been improved significantly. The contact angles of O_8H_2 and O_8H_2D were found to be 28.2° and 28.8°, respectively (Fig. S4), indicating that both hydrogels had good hydrophilic properties.

3.4. Tribology and tissue adhesion properties of OHA/HTCCMA hydrogels

Injury to articular cartilage is often accompanied by an increase in the COF of the cartilage surface, and implantation or injection of the external compounds could affect the lubrication properties of the joint, which consequently exacerbates the damage if the lubrication properties are not improved. The effect of the hydrogels in lubricating the interface between cartilage and a polished titanium plate (Fig. S5) was investigated using a custom-made setup in a tribometer (Fig. 4A and B). It can be seen that the OHA/HTCCMA hydrogel with or without cross-linking exhibited better lubrication than the blank group (0.9 % NaCl solution) and the control group (1 % HA solution, conventionally used in the clinic) (Fig. 4C). The COF values of O_8H_2 and O_8H_2D can be reduced to 0.065 and 0.078, respectively (compared to 0.041 for 4 % OHA and 0.109 for 1 % HTCCMA), which is much lower than 0.149 for 0.9 % NaCl solution and 0.096 for 1 % HA solution. This may be attributed to the high content of OHA in the hydrogel, and the results demonstrated that 4 % OHA solution is better than 1 % HA solution in terms of lubrication effect. This is because, during the preparation of OHA, the HA molecular chain was broken by sodium periodate, resulting in a smaller molecular weight of OHA than HA. The OHA with lower molecular weight can be dissolved in a higher concentration compared to the conventional high molecule weight HA under the same condition. Rowena [32] suggested that if polysaccharides act as a boundary lubricant in natural joints, they must be anchored to the surface either chemically or by specific means. OHA could be immobilized *via* Schiff base reaction between the aldehyde groups in OHA and amino groups on the cartilage surface, as well as the electrostatic interactions and hydrogen bonding between the hydrogel and cartilage surface, and the lubricating effect of OHA is consistent with their argument. It is expected that the OHA/HTCCMA hydrogel contains a large amount of unreacted aldehyde groups and charged groups (*e.g.* amino group, quaternary ammonium group and carboxylate group), which promotes the adhesion of the hydrogel to the cartilage surface (see tissue adhesion results below). As a result, the hydrogel can form a lubricating layer similar to the synovial fluid on the cartilage surface, and provide a stable lubricating effect superior to HA

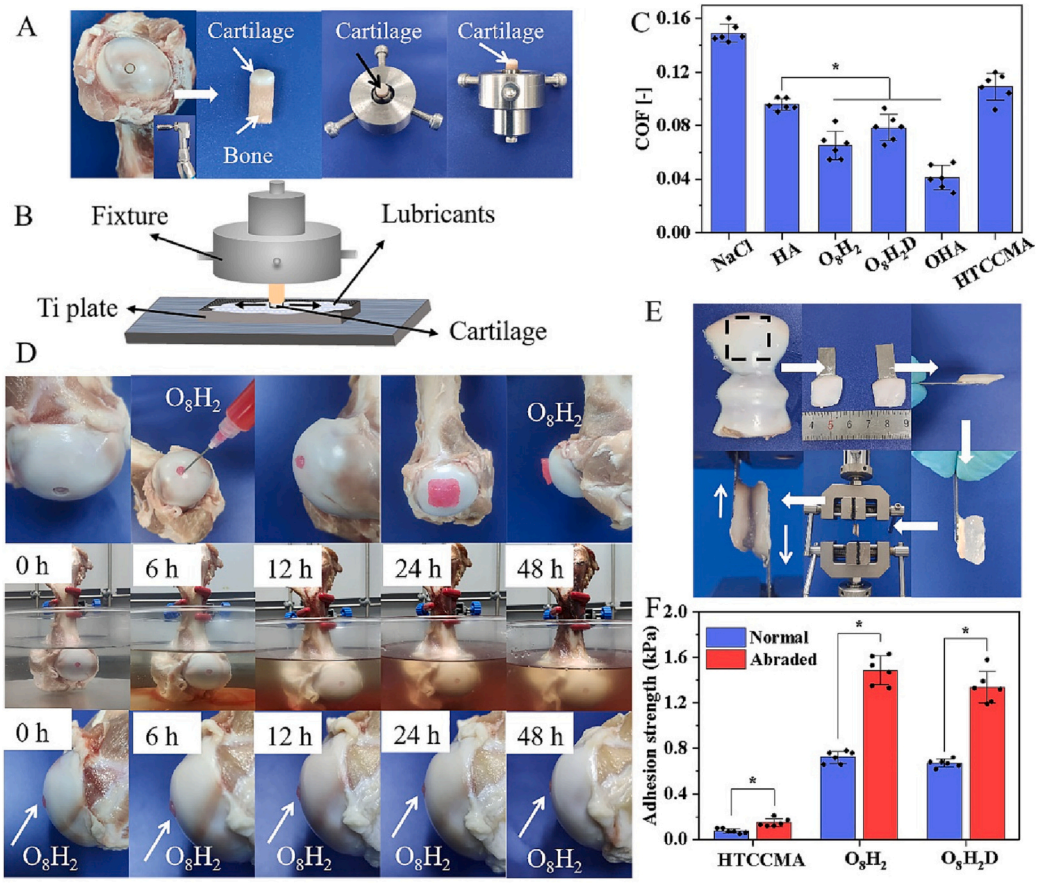

Fig. 4. Tribology of OHA/HTCCMA hydrogels and their adhesion evaluation. A) A cylindrical bone structure with a 4 mm diameter was drilled at the femoral head location using an osteotome. The bone structure was fixed using a custom-made fixture with the cartilage part exposed as the friction head. B) Schematical illustration of the friction test performed with a customized fixture to fix the bone structure as the friction head and a polished titanium plate as the base plate, and the hydrogel was added to the contact surface as lubricants. C) The COF values were obtained with different materials as lubricants: 0.9 % NaCl solution, 1 % HA solution, 4 % OHA solution, and 1 % HTCCMA solution (n = 6). D) A 5-mm diameter cavity was drilled in the surface of the femoral head, filled with O_8H_2 hydrogel, and immersed in PBS solution over 48 h at room temperature. E) A 10 × 10 mm cartilage surface was taken from the flat part of the medial and lateral femoral condyles of the femur, and glued using ethyl α-cyanoacrylate instantaneous adhesive onto a titanium sheet with the cartilage surface exposed. The two pieces of cartilage were adhered face to face using hydrogel. The setup was fixed on a tensile machine tester, and stretched at 10 mm/min, and tensile stresses were recorded. F) Adhesion strength of hydrogels to cartilage surface (n = 6). * represents $p < 0.05$.

alone. The dually cross-linked O_8H_2D hydrogel, on the other hand, showed a decrease in the lubrication effect compared to the O_8H_2 hydrogel, probably because of the increase in the overall mechanical strength of the cross-linked hydrogel. Nevertheless, it still showed a better lubrication effect than that of pure HA. The pure HTCCMA polymer increased the mechanical strength of OHA/HTCCMA hydrogel, but it lacked the water retention ability as OHA, and exhibited a low lubricating effect.

To investigate the adhesion performance of OHA/HTCCMA hydrogel on cartilage, a cartilage defect area with a diameter of about 5 mm was created on the joint head of a porcine femur, and it was coated with a layer of OHA/HTCCMA hydrogel (O_8H_2) and soaked in physiological saline (Fig. 4D and Fig. S6). As can be seen, the O_8H_2 hydrogel adhered stably at the defect area in an aqueous environment at pH 7.4 for up to 48 h (Fig. 4D). The synovial fluid would change to acidic (pH of ~6.4) in an OA patient [33], but the hydrogel maintained its adhesiveness on cartilage in the acidic condition for up to 12 h (Fig. S6). A lap shear test was also performed to quantify the adhesion strength of OHA/HTCCMA hydrogel on cartilage (Fig. 4E). The results showed that the OHA/HTCCMA hydrogel did have some adhesion effect on cartilage surface, and it showed an increase in adhesion strength on the abraded cartilage surface. The average adhesion strength of O_8H_2 hydrogel to normal and worn cartilage was 0.72 kPa and 1.49 kPa, respectively, and those of O_8H_2D hydrogel were 0.67 kPa and 1.34 kPa, respectively (Fig. 4F). In addition, it was found that the adhesion strength of the hydrogel changed with the change in OHA content (Fig. S7), indicating that the aldehyde groups in OHA played an important role in the adhesion of hydrogel by reacting with the amino groups in glycosaminoglycans in cartilage surface. The overall adhesion strength of the hydrogels to cartilage tissue was moderate. The slight adhesion of hydrogel to cartilage may be beneficial for joint lubrication as a high adhesion strength may not be conducive to the hydrogel diffusion and distribution in the joint cavity after injection, and may cause a braking effect on the patient's normal walking and affect knee health [34].

3.5. Antibacterial properties

Surgical treatment of joint diseases is often accompanied by the risk of secondary infection, and joint cavity injections are no exception. The antibacterial property of OHA/HTCCMA hydrogels was evaluated using Gram negative *E. coli* and Gram positive *S. aureus*. Both of the O_8H_2 and O_8H_2D hydrogels showed good inhibitory effects against the bacteria (Fig. 5A), and the inhibitory efficacy increased with time of incubation. After incubation for 24 h, the bactericidal efficacy of O_8H_2 against *E. coli* and *S. aureus* was determined to be 76.80 % and 95.90 %, respectively, and those of O_8H_2D was 74.52 % and 94.88 %, respectively (Fig. 5B). The antibacterial property was largely attributed to the presence of quaternary ammonium groups in the hydrogels.

3.6. Cytotoxicity and hemolysis

Since the OHA/HTCCMA hydrogel would deswell after incubation (Fig. 2B) and the deswelling may affect the adhesion and growth of cells on the hydrogel surface, test on extract method in according to the ISO 10993-5 standard was used for cytotoxicity evaluation. Rabbit articular chondrocytes (CP002) and bone marrow mesenchymal stem cells (BMSC) were used to evaluate the cytotoxicity and cell proliferation activity of the OHA/HTCCMA hydrogel. The results showed (Fig. 6A and B) that the OHA/HTCCMA hydrogel extract obtained with an extracting ratio of 80 μg/mL and below had a cell growth-promoting effect, with the most pronounced promoting effect at 40 μg/mL. A slight cytostatic effect was observed at the ratio of 100 μg/mL. The hydrogel extract obtained at the extracting ratio of 40 μg/mL was selected for further study of the cell proliferation effect (Fig. 6C and D). The extracts from O_8H_2 and O_8H_2D hydrogels showed a significant pro-cell proliferation effect compared with the culture medium control, with a significant difference on the fifth day observed. This phenomenon may be attributed to that HA released from the hydrogel in the extraction process (Fig. 2E), which contributes to the cell proliferation of chondrocytes and BMSCs. It was also evident from the live/dead staining results (Fig. S8) that the O_8H_2 and O_8H_2D hydrogels had a significant pro-value-added effect on chondrocytes and did not cause apoptosis. A hemolysis test on OHA/HTCCMA hydrogel was performed (Fig. 6E and F), and it was found that neither OHA/HTCCMA hydrogel nor the individual polymer components (OHA and HTCCMA) at the concentrations had a significant hemolytic effect on red blood cells, indicating that OHA/HTCCMA hydrogel does not affect the internal environmental homeostasis of the body.

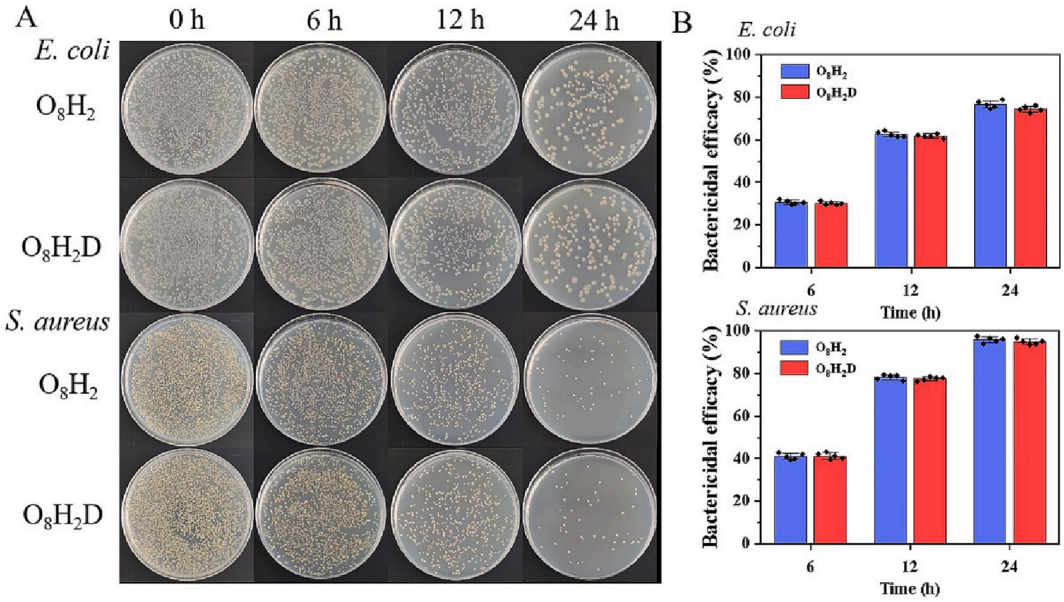

Fig. 5. Antibacterial property. A) Photographs of bacterial colonies on culture plates after incubation with hydrogels for 6, 12 and 24 h. B) Bactericidal efficacy of hydrogels after incubation for 6, 12 and 24 h ($n = 5$).

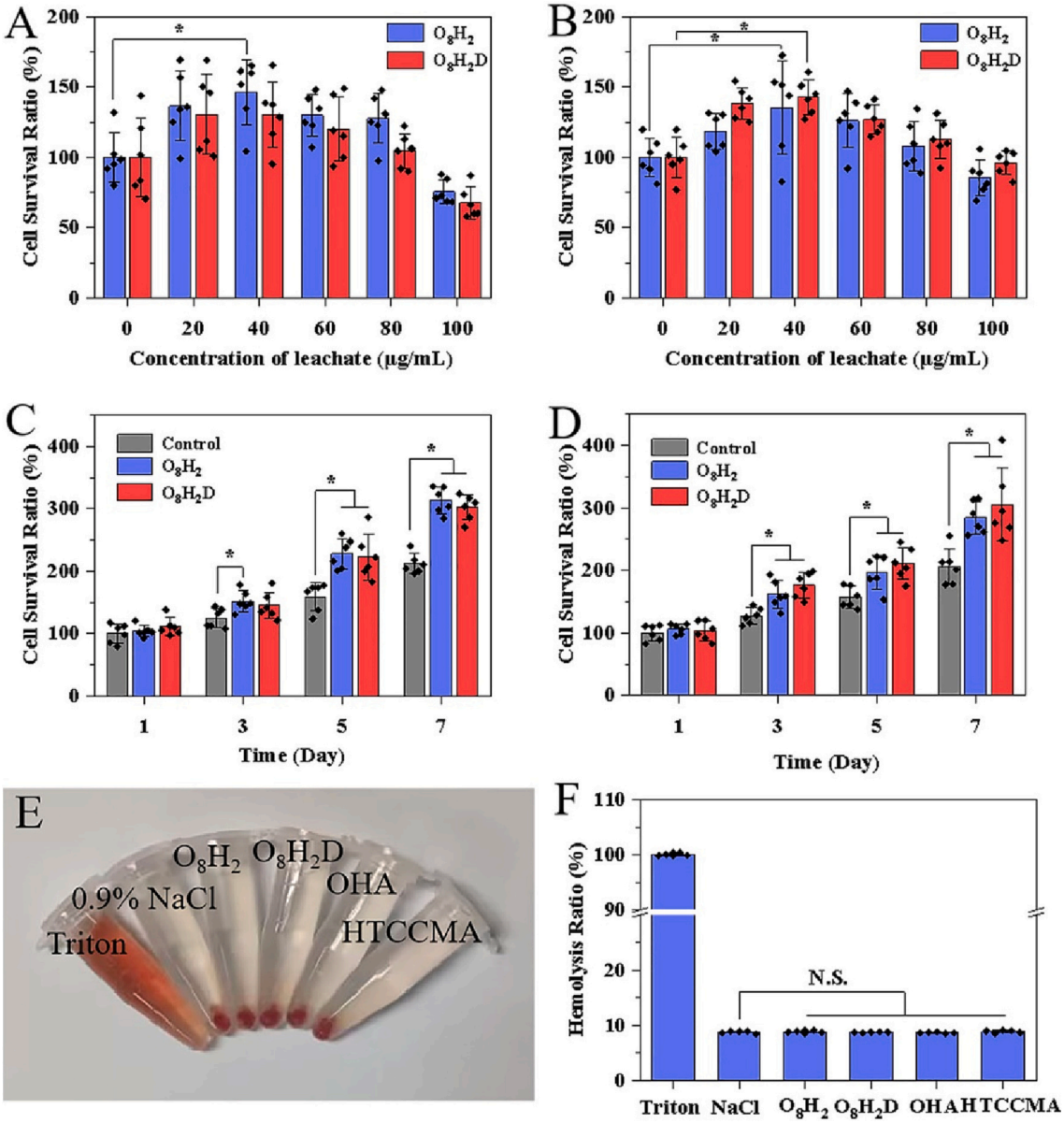

Fig. 6. Cytotoxicity and hemolysis of hydrogels. A) Cytotoxicity of hydrogel extracts at different concentrations against CP002 (n = 6). B) Cytotoxicity of hydrogel extracts at different concentrations against BMSC (n = 6). C) Effect of 40 μg/mL of hydrogel extract on the cell proliferation of CP002 (n = 6). D) Effect of 40 μg/mL of hydrogel extract on the cell proliferation of BMSC (n = 6). * represents $p < 0.05$. E) Photographs of the hemolytic effect, and F) hemolysis ratio of Triton X-100 (positive group), 0.9 % NaCl (negative group), and the various hydrogels (n = 5). N.S. represents non-significant difference.

3.7. In vivo animal study

The *in vivo* biocompatibility and degradation properties of OHA/HTCCMA hydrogel were investigated by subcutaneous implantation in rabbits. The results showed (Fig. 7) that the OHA/HTCCMA hydrogel either with or without photo-cross-linking could be completely degraded and absorbed within 28 days. Tissue section staining showed that there was no inflammatory reaction. It was also observed that the degradation rate of the dually cross-linked O_8H_2D hydrogel was slower compared to the dynamic cross-linked O_8H_2 hydrogel. The prolonged degradation effect of the hydrogel may be beneficial for maintaining its therapeutic effect in the body.

A cartilage defect model of rabbit femoral talus was established to investigate the cartilage-repairing effect of the OHA/HTCCMA hydrogel. The results showed (Fig. 8A) that the O_8H_2 and O_8H_2D groups contained hydrogel in the wound on Day 1, while the blank control wound was filled with bruises. At 14 days, that the osteogenic part of the wound had been almost closed in both the O_8H_2 and O_8H_2D hydrogel groups, and a layer containing white tissue was observed on the surface of the wound area, which was probably due to the migration of chondrocytes to the osteogenic surface as well as the production of collagen fibers. In addition, the cartilaginous portion was shrinking toward the center of the wound in the O_8H_2D hydrogel group. The H&E staining results (Fig. 8B) showed that there was a large vacancy in the osteogenic portion of the control group, whereas both the wounds in the O_8H_2 and O_8H_2D hydrogel groups were closed, with a full osteogenic structure observed. The Modified Saffron-O and Fast Green staining showed a small number of red dots in the tissue of the O_8H_2D hydrogel group (Fig. 8C), indicating that there was a small amount of migrating cartilage tissue in the area. The results from Masson's Trichrome staining (Fig. S9A) showed that there was collagen fiber production in the osteogenic portion of the O_8H_2 and O_8H_2D hydrogel groups, indicating that both hydrogels promoted the production of collagen fibers, which was beneficial for the cartilage repair process. After 28 days, a

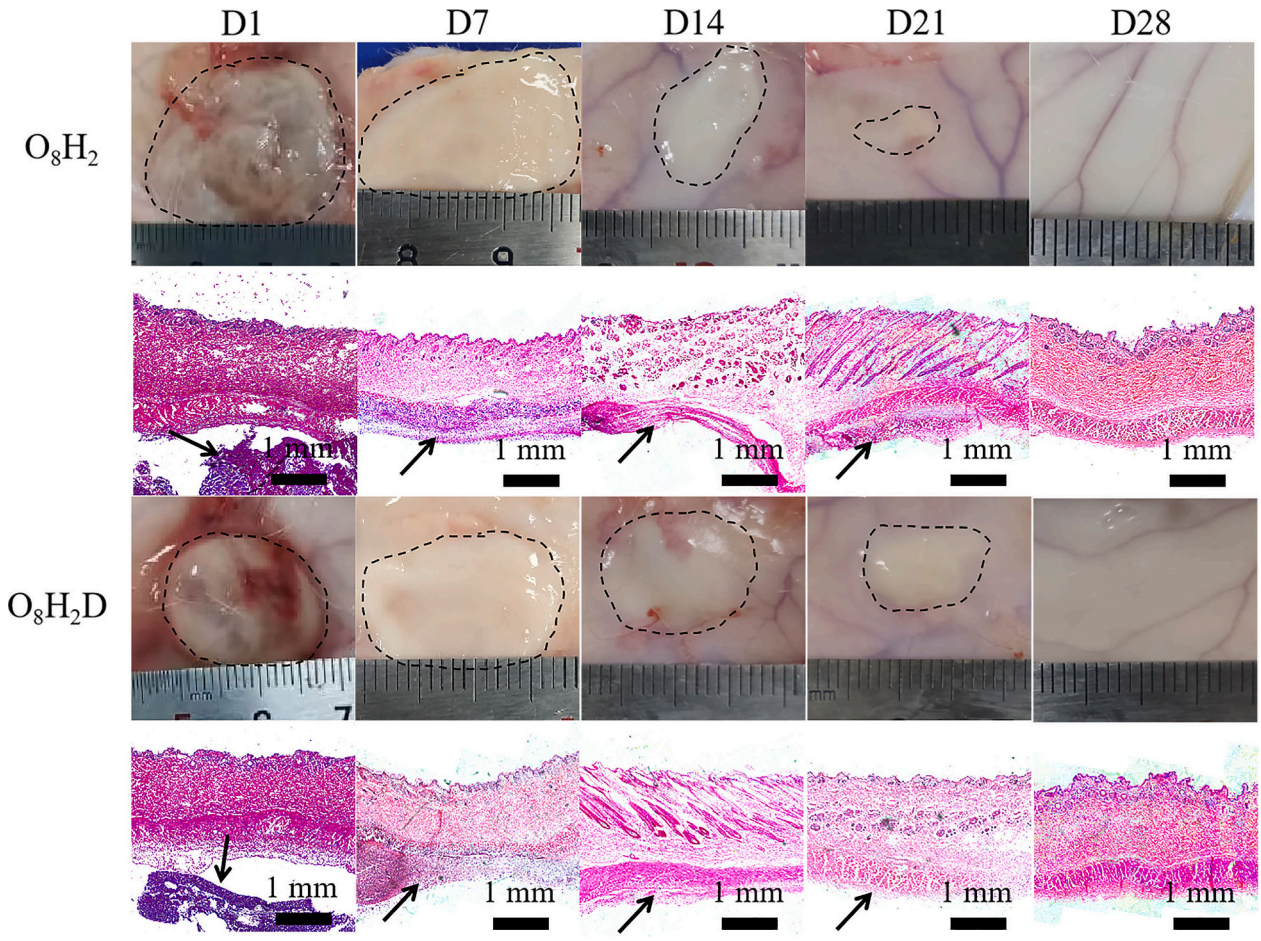

Fig. 7. Subcutaneous degradation and histocompatibility of O_8H_2 and O_8H_2D hydrogels after subcutaneous implantation in rabbits for 28 days. The areas in the dashed line and the black arrows indicated the remaining hydrogel.

superficial look reveals (Fig. 8A) that the osteogenic portion of all the three groups had been closed, and although the hydrogels had been degraded by this time, there is a significant inward contraction of the cartilage layer in the O_8H_2 and O_8H_2D hydrogel groups. It is possible that the positive effect of the hydrogel on the wound initiated the repair process. After 42 days, the wounds of the O_8H_2 and O_8H_2D hydrogel groups had been fully closed, and the control group started to shrink inward. From the H&E results (Fig. 8B), it can be seen that without gel filling in the tissue defect of the control group, the healing process was mainly osteogenic regeneration, resulting in a tissue structure containing a large number of osteoblasts but few cartilage structure and collagen formation (Fig. 8C and Fig. S9). In contrast, the O_8H_2 and O_8H_2D hydrogel groups showed a cartilage-repairing effect, probably due to the spatial filling of three-dimensional hydrogel gel in the wounds acted like an extracellular matrix, which provided spatial support as well as a suitable microenvironment for the migration and growth of chondrocytes around the defect to the wound, and allowing chondrocytes to maintain their morphology and promote cartilage structure formation. The results of Saffron-O and Fast Green staining (Fig. 8C) and Toluidine Blue staining (Fig. S9B) showed that a large amount of cartilage structure was generated on the surface, while the control group only has inwardly contracted bony structure with no obvious matured cartilage structure. The O_8H_2D hydrogel group had a greater amount of collagen production than the O_8H_2 hydrogel group (Fig. S9A), and showed a better repairing effect. After 56 days (Fig. 8A), there was an arthritis-like structure on the cartilage surface of the control group. Significant cellular abnormalities and weak staining were seen in the Saffron-O and Fast Green staining images (Fig. 8C), and significant bony repair was seen in Masson's Trichrome staining images (Fig. S9A) and Toluidine Blue cartilage stain images (Fig. S9B), indicating that the absence of tissue filling gel was detrimental to cartilage tissue repair and that bone formation was present without regeneration of cartilage structures. The wounds in the O_8H_2 and O_8H_2D hydrogel groups were completely closed. Compared to the O_8H_2 hydrogel group, where the cartilage structure differed from the surrounding cartilage structure and was still far from perfect repair, the cartilage surface of the O_8H_2D hydrogel group had reached a good level of repair, and the healed structure was comparable to the surrounding cartilage, and the surface was smooth. A complete cartilage structure can be seen in the Saffron-O and Fast Green staining image (Fig. 8C) and the Toluidine Blue cartilage staining image (Fig. S9B). A small number of collagen fibers can be found in the osteogenic portion of the Masson's Trichrome staining image of the O_8H_2 and O_8H_2D group (Fig. S9A), which may be caused by the osteogenic structures encasing some of the collagen fibers in the process of mature cancellous bone formation, which also indicates that the hydrogels can promote the production of collagen fibers.

Overall, the OHA/HTCCMA hydrogel group showed significantly better collagen production and cartilage repair performance than the control group over the 56-day treatment period. The photo-cross-linked O_8H_2D hydrogel showed superior therapeutic effects compared to the dynamic cross-linked O_8H_2 hydrogel. This indicates that the photo-cross-linked OHA/HTCCMA hydrogel is beneficial in the cartilage repair process, which we speculate could be attributed to the fact that the photo-cross-linked hydrogel slows down the degradation rate of hydrogel and prolongs the therapeutic time. In addition, the photo-cross-linked hydrogel has a closer mechanical strength to the cartilage

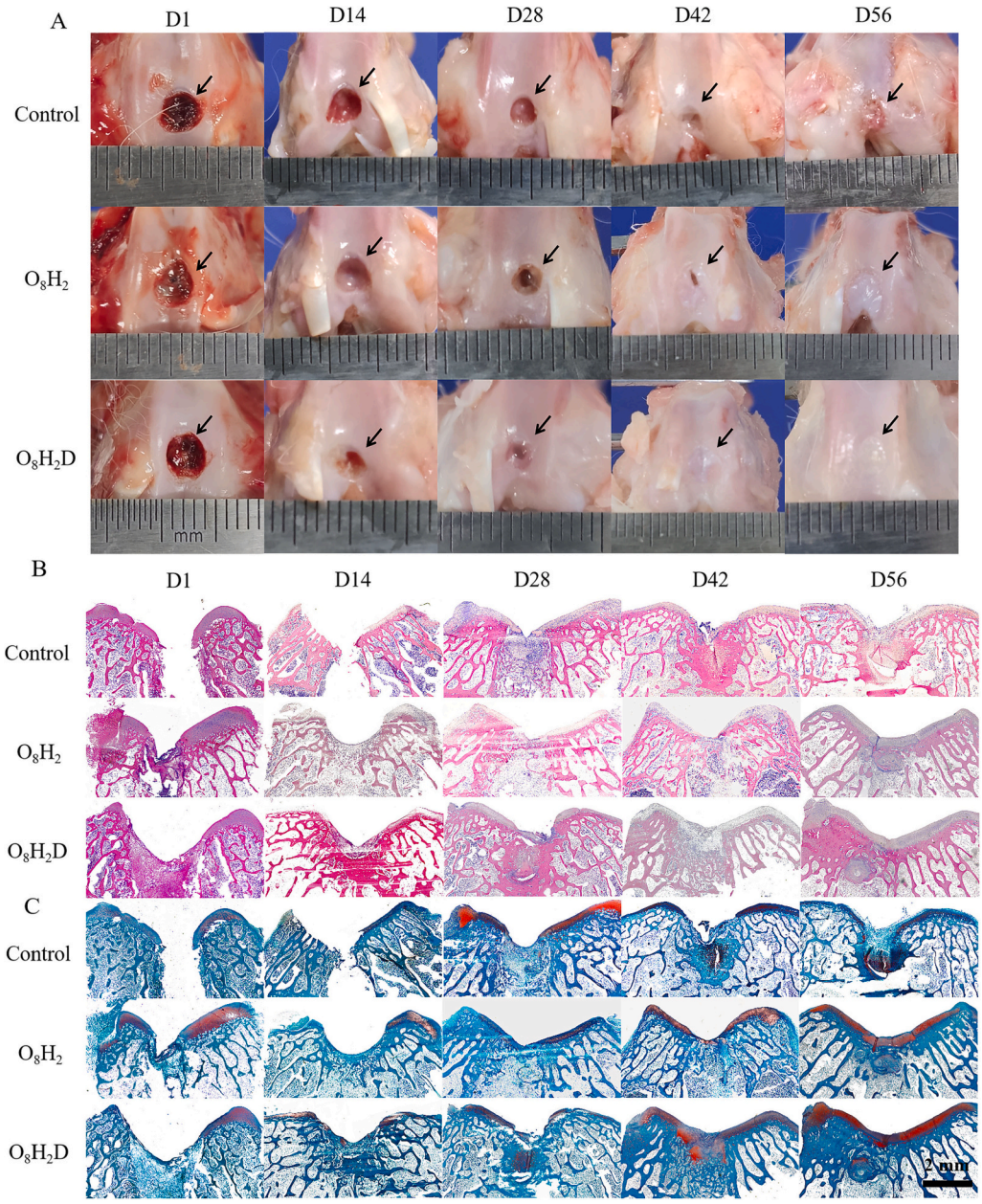

Fig. 8. Cartilage-repairing effect of hydrogels. A) Photographs of the gross appearance of the healed cartilage in rabbit joints over 56 days. B) H&E staining, and C) Modified Saffron-O and Fast Green staining images of the cartilage tissue.

and is suitable for chondrocyte growth.

4. Conclusions

In this study, a dynamically cross-linked polysaccharide hydrogel based on oxidized hyaluronic acid (OHA) and *N*-(2-hydroxypropyl)-3-trimethylammonium chitosan chloride (HTCC) methacrylate (HTCCMA) was fabricated *via* the Schiff base reaction. The dynamic hydrogel was further cross-linked *via* photo-irradiation to obtain a dually cross-linked hydrogel with enhanced mechanical properties. The OHA/HTCCMA hydrogel exhibited excellent lubrication, which was attributed to the strong water retention capacity of the large amount of OHA in the hydrogel, forming a lubricating layer on the cartilage surface. The OHA/HTCCMA hydrogel also formed dynamic covalent bonds *via* Schiff base reaction between the OHA components and the glycosaminoglycans on the cartilage surface to achieve good tissue adhesion and prevent detachment from the tissue defect. In addition, the hydrogel showed good antibacterial property due to the presence of quaternary ammonium groups in the HTCCMA component of the hydrogel. Cellular experiments demonstrated that the hydrogel had a value-added promoting effect on the proliferation of both chondrocytes and BMSC. *In vivo* studies confirmed that the hydrogel had good tissue compatibility and controllable degradation rate, and was effective in promoting cartilage regeneration and preventing cartilage lesions in a rabbit femoral defect model. However, the mechanism of hydrogel-induced cartilage repair is currently unknown, and the mechanical properties of newly formed cartilage compared to normal cartilage need to be investigated in the future work. In summary, this work developed a lubricious and adhesive antimicrobial hydrogel with desirable bioactivity for effectively addressing cartilage defects in joint injuries, thus providing a promising solution for degenerative cartilage diseases such as osteoarthritis.

CRediT authorship contribution statement

Haofeng Qiu: Conceptualization, Methodology, Investigation, Data curation, Writing – original draft. **Junjie Deng:** Methodology, Data curation. **Rufang Wei:** Methodology, Data curation. **Xiang Wu:** Methodology. **Shengjia Chen:** Methodology. **Yanyu Yang:** Methodology. **Chenyang Gong:** Investigation. **Lingling Cui:** Investigation. **Zhangyong Si:** Investigation, Methodology. **Yabin Zhu:** Writing – review & editing. **Rong Wang:** Conceptualization, Methodology, Writing – review & editing, Supervision. **Dangsheng Xiong:** Conceptualization, Methodology, Writing – review & editing, Supervision.

Declaration of competing interest

The authors declare no conflicts of interest.

Data availability

Data will be made available on request.

Acknowledgements

This work was supported by the National Key Research and Development Program of China (2018YFE0119400), National Natural Science Foundation of China (51975296), Youth Innovation Promotion Association CAS (2021296), Key Research and Development Program of Ningbo (2022Z132), and Foundation of Director of Ningbo Institute of Materials Technology and Engineering CAS (2021SZKY0301).

Appendix A. Supplementary data

Supplementary data to this article can be found online at https://doi.org/10.1016/j.ijbiomac.2023.125249.

References

[1] A.R. Armiento, M. Alini, M.J. Stoddart, Articular fibrocartilage - why does hyaline cartilage fail to repair? Adv. Drug Deliv. Rev. 146 (2019) 289–305.
[2] T. Simon, D. Jackson, Articular cartilage: injury pathways and treatment options, Sports Med. Arthrosc. Rev. 26 (2018) 31–39.
[3] Y. Krishnan, A.J. Grodzinsky, Cartilage diseases, Matrix Biol. 71-72 (2019) 51–69.
[4] A.R. Armiento, M.J. Stoddart, M. Alini, D. Eglin, Biomaterials for articular cartilage tissue engineering: learning from biology, Acta Biomater. 65 (2018) 1–20.
[5] M. Voga, G. Majdic, Articular cartilage regeneration in veterinary medicine, Adv. Exp. Med. Biol. 1401 (2022) 23–55.
[6] J. Yang, Y.S. Zhang, K. Yue, A. Khademhosseini, Cell-laden hydrogels for osteochondral and cartilage tissue engineering, Acta Biomater. 15 (2017) 1–25.
[7] A.R. Watkins, H.L. Reesink, Lubricin in experimental and naturally occurring osteoarthritis: a systematic review, Osteoarthr. Cartil. 28 (2020) 1303–1315.
[8] L. Rojo, Combination of polymeric supports and drug delivery systems for osteochondral regeneration, Adv. Exp. Med. Biol. 1059 (2018) 301–313.
[9] R. Papalia, E. Albo, F. Russo, A. Tecame, G. Torre, S. Sterzi, F. Bressi, V. Denaro, The use of hyaluronic acid in the treatment of ankle osteoarthritis: a review of the evidence, J. Biol. Regul. Homeost. Agents 27 (2017) 91–102.
[10] H.J. Faust, S.D. Sommerfeld, R. Sona, R. Andrew, R. Sangeeta, B. Tsui, P. Martin, M.L. Amzel, S. Anirudha, E. Jennifer, A hyaluronic acid binding peptide-polymer system for treating osteoarthritis, Biomaterials. 183 (2018) 93–101.
[11] Y. Liu, L. Peng, L. Li, C. Huang, K. Shi, X. Meng, P. Wang, M. Wu, L. Li, H. Cao, 3D-bioprinted BMSC-laden biomimetic multiphasic scaffolds for efficient repair of osteochondral defects in an osteoarthritic rat model, Biomaterials. 279 (2021), 121216.
[12] F.X. Zhang, P. Liu, W. Ding, Q.B. Meng, D.H. Su, Q.C. Zhang, R.X. Lian, B.Q. Yu, M. Zhao, J. Dong, Injectable mussel-inspired highly adhesive hydrogel with exosomes for endogenous cell recruitment and cartilage defect regeneration, Biomaterials 278 (2021), 121169.
[13] J. Shin, E.H. Kang, S. Choi, E.J. Jeon, S.W. Cho, Tissue-adhesive chondroitin sulfate hydrogel for cartilage reconstruction, ACS Biomater. Sci. Eng. 13 (2021) 4230–4243.
[14] M.L. Vainieri, A. Lolli, N. Kops, D. D'Atri, D. Eglin, A. Yayon, M. Alini, S. Grad, K. Sivasubramaniyan, G.V. Osch, Evaluation of biomimetic hyaluronic-based hydrogels with enhanced endogenous cell recruitment and cartilage matrix formation, Acta Biomater. 1 (2020) 293–303.
[15] K.D. Ngadimin, A. Stokes, P. Gentile, A.M. Ferreira, Biomimetic hydrogels designed for cartilage tissue engineering, Biomater. Sci. 15 (2021) 4246–4259.
[16] W. Wei, H. Dai, Articular cartilage and osteochondral tissue engineering techniques: recent advances and challenges, Bioact. Mater. 6 (2021) 4830–4855.
[17] M. Hafezi, K.S. Nouri, M. Zare, N.R. Esmaeely, P. Davoodi, Advanced hydrogels for cartilage tissue engineering: recent progress and future directions, Polymers. 30 (2021) 4199.
[18] W. Zhang, Y. Jiang, H. Wang, Q. Li, K. Tang, In situ forming hydrogel recombination with tissue adhesion and antibacterial property for tissue adhesive, J. Biomater. Appl. 37 (2022) 12–22.
[19] C. Li, Z. Cao, W. Li, R. Liu, Y. Liu, A review on the wide range applications of hyaluronic acid as a promising rejuvenating biomacromolecule in the treatments of bone related diseases, Int. J. Biol. Macromol. 165 (2020) 1264–1275.
[20] D.P. Maleki, J. Hallajzadeh, Z. Asemi, M.A. Mansournia, B. Yousefi, Chitosan applications in studying and managing osteosarcoma, Int. J. Biol. Macromol. 1 (2021) 321–329.
[21] Y. Lei, X. Wang, J. Liao, J. Shen, Y. Li, Z. Cai, N. Hu, X. Luo, W. Cui, W. Huang, Shear-responsive boundary-lubricated hydrogels attenuate osteoarthritis, Bioact. Mater. 20 (2022) 472–484.
[22] A. Avenoso, A. D'Ascola, M. Scuruchi, G. Mandraffino, A. Calatroni, A. Saitta, S. Campo, G.M. Campo, Hyaluronan in experimental injured/inflamed cartilage: in vivo studies, Life Sci. 15 (2018) 132–140.
[23] X. Pang, W. Li, L. Chang, J.E. Gautrot, H.S. Azevedo, Hyaluronan (HA) immobilized on surfaces via self-assembled monolayers of HA-binding peptide modulates endothelial cell spreading and migration through focal adhesion, ACS Appl. Mater. Interfaces 9 (2021) 25792–25804.
[24] L.J. Kang, J. Yoon, J.G. Rho, H.S. Han, W. Kim, Self-assembled hyaluronic acid nanoparticles for osteoarthritis treatment, Biomaterials. 275 (2021), 120967.
[25] M.A. Matica, F.L. Aachmann, A. Tndervik, H. Sletta, V. Ostafe, Chitosan as a wound dressing starting material: antimicrobial properties and mode of action, Int. J. Mol. Sci. 24 (2019) 5889.
[26] P. Li, L. Fu, Z. Liao, Y. Peng, C. Ning, C. Gao, D. Zhang, X. Sui, Y. Lin, S. Liu, C. Hao, Q. Guo, Chitosan hydrogel/3D-printed poly(ε-caprolactone) hybrid scaffold containing synovial mesenchymal stem cells for cartilage regeneration based on tetrahedral framework nucleic acid recruitment, Biomaterials. 278 (2021), 121131.
[27] Z. Cai, M. Hong, L. Xu, K. Yang, K.Y. Chiu, Prevent action of magnoflorine with hyaluronic acid gel from cartilage degeneration in anterior cruciate ligament transection induced osteoarthritis, Biomed. Pharmacother. 126 (2020), 109733.
[28] X. Zhao, B. Guo, H. Wu, Y. Liang, P.X. Ma, Injectable antibacterial conductive nanocomposite cryogels with rapid shape recovery for noncompressible hemorrhage and wound healing, Nat. Commun. 17 (2018) 2784.
[29] C. Han, H. Zhang, Y. Wu, X. He, X. Chen, Dual-crosslinked hyaluronan hydrogels with rapid gelation and high injectability for stem cell protection, Sci. Rep. 14 (2020) 14997.
[30] K. Fang, Q. Gu, M. Zeng, Z. Huang, H. Qiu, J. Miao, Y. Fang, Y. Zhao, Y. Xiao, T. Xu, R.P. Golodok, V.V. Savich, A.P. Ilyushchenko, F. Ai, D. Liu, R. Wang, Tannic acid-reinforced zwitterionic hydrogels with multi-functionalities for diabetic wound treatment, J. Mater. Chem. B 8 (2022) 4142–4152.
[31] G. Lan, S. Zhu, D. Chen, H. Zhang, L. Zou, Y. Zeng, Highly adhesive antibacterial bioactive composite hydrogels with controllable flexibility and swelling as wound dressing for full-thickness skin healing, Front. Bioeng. Biotechnol. 23 (2021), 785302.
[32] C. Rowena, Friction and adhesion of polysaccharides, Tribol. Online 9 (2014) 154–163.
[33] A.F. Lombardi, Y. Ma, H. Jang, S. Jerban, Q. Tang, A.C. Searleman, R.S. Meyer, J. Du, E.Y. Chang, AcidoCEST-UTE MRI reveals an acidic microenvironment in knee osteoarthritis, Int. J. Mol. Sci. 23 (2022) 4466.
[34] M. Sukopp, F. Sukopp, S.P. Hacker, A. Ignatius, L. Dürselen, A.M. Seitz, Influence of menisci on tibiofemoral contact mechanics in human knees: a systematic review, Front. Bioeng. Biotechnol. 3 (2021), 765596.